Available online at www.sciencedirect.com
SCIENCE DIRECT®
International Journal of Mass Spectrometry 235 (2004) 179–186
International Journal of Mass Spectrometry
www.elsevier.com/locate/ijms

Argon clusters produced in a nozzle beam at low pressure: Ar_2 ionisation cross-section measurement

J.L. Jauberteau*, I. Jauberteau, J. Aubreton

SPCTS, UMR 6638 CNRS, UER des Sciences, 123 av A. Thomas, 87060 Limoges, France

Received 23 March 2004; accepted 5 May 2004

Available online 9 June 2004

Abstract

This work is devoted to the study of the ionisation process of Ar_2 neutral cluster producing Ar_2^+. First we characterize the experimental set-up working at low pressure and we show that in these experiments the Ar_2^+ ion is mainly produced by the direct ionisation of Ar_2 rather than associative ionisation processes, neutral clusters dissociative ionisation processes or ion clusters decay processes. Using an alternate approach to the microscopic Deutsch–Märk formalism, we have measured the absolute value of the electron impact ionisation cross-section of Ar_2 producing Ar_2^+ ion at low electron energy ranges from 0 to 32 eV. These results are compared with values proposed in the literature.

Finally, using these ionisation cross-section values, it is possible to measure the partial pressure of Ar and Ar_2 downstream the expansion jet and to compare these pressure values to the total pressure value of argon. The relative dimer argon pressure is about 0.5% the total pressure in the expansion chamber when the stagnation pressure in the chamber before the expansion is 1100 Pa.

Keywords: Ionisation cross-section; Nozzle beam; Expansion jet; Cluster; Argon cluster; Argon dimer

1. Introduction

When a gas expands out of a nozzle into the vacuum its random thermal energy is converted into directed kinetic energy in a supersonic flow. The expansion is adiabatic and subsequent cooling to a supersaturated state undergoes producing clusters where the atoms or molecules are held together by the van der waals forces [1–4]. Clusters offer a means by which to bridge the gap between the gaseous and condensed phase so that the details of condensation and nucleation phenomena can be probed at the molecular level [3]. Moreover, due to their high saturation energy and their rather simple excitation mechanisms excimers are the ideal media for high power lasers in the UV. The shortest wavelength at which gain may be achieved is emitted by the Ar_2 dimer [5].

The purpose of this work is to study the electron impact ionisation of Ar_2 producing Ar_2^+ and to measure the absolute ionisation cross-section value of this process.

* Corresponding author. Tel.: +33 555 45 75 03; fax: +33 555 45 72 11.
E-mail address: jauberteau-ijl@unilim.fr (J.L. Jauberteau).

1387-3806/$ – see front matter © 2004 Elsevier B.V. All rights reserved.
doi:10.1016/j.ijms.2004.05.001

2. Experimental details

The experimental set-up is schematically shown in the Fig. 1. It consists of a stainless steel tube used as a first vacuum chamber at the stagnation pressure P_1 and the temperature T_1. It is connected at right angle to a valve and a first vacuum pump group which is used to clean the chamber or to keep a constant pressure while experiments are performed. This group is composed with two units: first a turbo molecular pump (210 l/s in N_2) with a primary pump Alcatel (10 m^3/h) used to clean the reactor tube before experiments and second a Roots blower pump Alcatel (70 m^3/h) with a primary pump (60 m^3/h) Alcatel used when experiments are performed. The Roots pump is used in order to keep the pressure constant from 0 to 530 Pa at an adjustable constant drift velocity ranging between 0 and 30 m/s. The low flow can be achieved closing the valve placed between the vacuum chamber and the pump.

A nozzle (named B on the Fig. 1) with an aperture of 100 μm diameter is centred on the axis of the first vacuum chamber. It produces a supersonic expansion jet within a second vacuum chamber kept at a lower pressure P_2 and at the temperature T_2. This second vacuum chamber is pumped

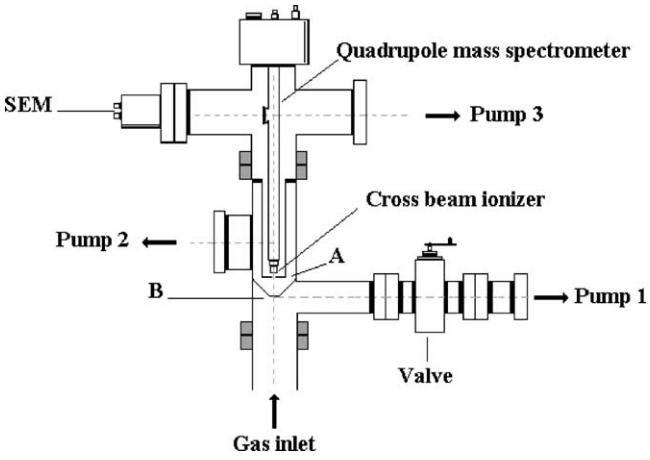

Fig. 1. Experimental set-up.

by means of a dry MD4 Balzers pump (3.6 m^3/h) and a Drag turbomolecular pump Balzers 260 (210 l/s in N_2). The mass spectrometer is placed on the axis of the two chamber and a hole 500 μm diameter (A) is drilled between the second vacuum chamber and the quadrupole chamber. In the quadrupole, the pressure is maintained at 10^{-3} Pa by means of a third vacuum pump group, composed with a small turbo molecular pump Tmu 065 Balzers (56 l/s in N_2) and a dry primary pump M22 Balzers (2.4 m^3/h).

The distance between A and B ranges between 4 and 5 cm and is of the order of the mean free path length in the second vacuum chamber maintained at a pressure of 0.1 Pa. The ionisation chamber contains an electron cross beam apparatus placed 5 mm above the 500 μm diameter hole and just before the mass spectrometer quadrupole (QMA 400 Balzers). The emission electron current is stabilized and ranges from 0 to 2 mA and the electron energy ranges from 0 to 125 eV. The experimental error performed on the electron energy value is about 0.2 eV. Before experiments, the filaments of the electron beam apparatus are heated for 1 h with a current intensity ranges between 0 and 3 A, in order to clean an evaporate all species previously deposited on the filaments. The ion signal is detected by means of a Faraday cup in the axis of the quadrupole or using a secondary electron multiplier (SEM) perpendicular to the axis. Each point presented in the different figures of this paper is the mean value calculated over 50 cycles data acquisitions. The estimated relative error performed on the mass spectrometer intensity values ranges between 5 and 10% according to the experimental conditions.

3. Results and discussions

According to Helm et al. [6], the molecular rare-gas ions observed by means of mass spectrometer may be produced either by the direct ionisation of the van der Waals (vdw) neutral dimer of the rare gas present in the beam after the nozzle B or by an associative ionisation process named the Hornbeck–Molnar process. This process is corresponding to a bimolecular collision involving an excited rare-gas atom R^* first produced by electron impact in the ionisation chamber. It can be written as:

$$R + e \rightarrow R^* + e$$

$$R^* + R \rightarrow R_2^+ + e$$

In this case, the dimer ion is produced by a three body collision process which can occur only if the pressure in the ionisation chamber is large enough. Helm et al. [6] have shown that for this process the signal intensity measured for the dimer ion is proportional to the square of the pressure in the quadrupole. This process is only efficient if the pressure in the first vacuum cell is low and if the pumping speed is throttling in the ion source. In our case, the pressure in the ionisation chamber is too low (10^{-2} Pa), the mean free path is too large (0.5–1 m) and a three body collision process cannot occur. Consequently, only the first ionisation process (direct ionisation of neutral dimer) can be observed in our case.

For the sake of clarity, the characterization of the expansion jet in the vacuum cell after the nozzle (B) is presented in the Appendix A placed at the end of this paper.

3.1. Qualitative results

The Fig. 2 shows the spectrum of mass spectrometer intensity versus the m/z ratio ranges between 0 and 150. This figure shows qualitative results and the signal intensity value reported on the graph is not a corrected signal of mass-dependent detection sensitivity of the mass spectrometer apparatus. The electron energy is equal to 18 eV and the pressure in the first cell is 1200 Pa. The spectrum shows peak located at $m/z = 17$, 18, 40 and 80 which can be ascribed to OH^+, H_2O^+, Ar^+ and $Ar_2{}^+$, respectively. The peak observed at $m/z = 80$ is vanished at argon pressure lower than 500 Pa. The peak at $m/z = 120$, corresponding to $Ar_3{}^+$ is not observed.

3.2. Threshold ionisation and ionisation cross-section of Ar_2 producing $Ar_2{}^+$ ion

The Fig. 3 shows the change in the signal intensity measured for $m/z = 40$ and 80 for Ar^+ and $Ar_2{}^+$, respectively, versus the electron energy used in the ionisation chamber. The curves are obtained using a polynomial interpolation. Results show that the threshold ionisation of $Ar_2{}^+$ is lower than the threshold ionisation of Ar^+. It is equal to 15.3 eV. This value is determined using the threshold ionisation of Ar^+ (15.75 eV [9,14]) as the reference to calibrate the electron energy scale. On the Fig. 3 data points and the threshold ionisation values proposed in the literature are reported. The appearance potential of $Ar_2{}^+$ determined in the case of the Hornbeck–Molnar process (H, M), ranges between 14.4 and 14.8 eV [6]. This value agree with the value determined by Hornbeck and Molnar (15.06 (±) 0.2 eV [6]) or Ng et al.

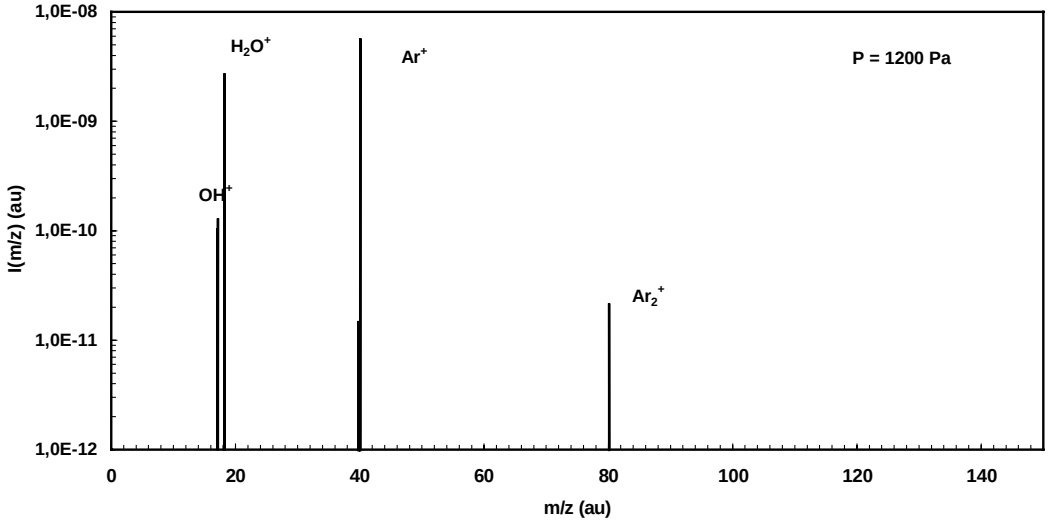

Fig. 2. Mass spectrometer spectrum intensity vs. the m/z ratio ranges between 0 and 150. The electron energy in the ionisation chamber is equal to 18 eV and the pressure in the first cell is 1200 Pa.

(14.54 (±) 0.02 eV). In our case the threshold ionisation value is 15.3 eV (±) 0.2 eV and corresponds to the value determined by Helm et al. [6] (15.2 (±) 0.2 eV), in the case of the electron impact ionisation process of the neutral dimer Ar_2 (0.6 eV above the threshold ionisation determined for the Hornbeck–Molnar process). This result confirms our previous assumption that in our case $Ar_2{}^+$ proceed via the direct ionisation of Ar_2.The mass spectrometer signal intensity I_i measured for i species in the case of a direct ionisation is given by [15,16]:

$$I_i = A\sigma(\varepsilon_e) I_b n_i = T_i \sigma(\varepsilon_e) n_i \tag{6}$$

where A is a factor depending on the sensitivity of the QMS and of the vacuum conductivity (transmission probability of particle) of the sample hole in the extractor, $\sigma(\varepsilon_e)$ is the ionisation cross-section at the electron energy ε_e, I_b is the electron current intensity in the cross beam and n_i is the i species concentration. T_i is the transmission factor $T_i = AI_b$ for the i species.

At a constant pressure in the vacuum cell and at a constant electron current intensity in the cross beam, the relative signal intensity measured for i species is given by:

$$\frac{I_i}{I_{i0}} = \frac{\sigma_i(\varepsilon_e)}{\sigma_i(\varepsilon_{e0})} \tag{7}$$

This equation shows that the relative electron impact ionisation cross-section of i species can be deduced from the relative mass spectrometer signal intensity measured for the same species. In this relation I_{i0} is the signal intensity measured at an electron energy equal to ε_{e0}. In order to check the accuracy of our measurements, we have measured the

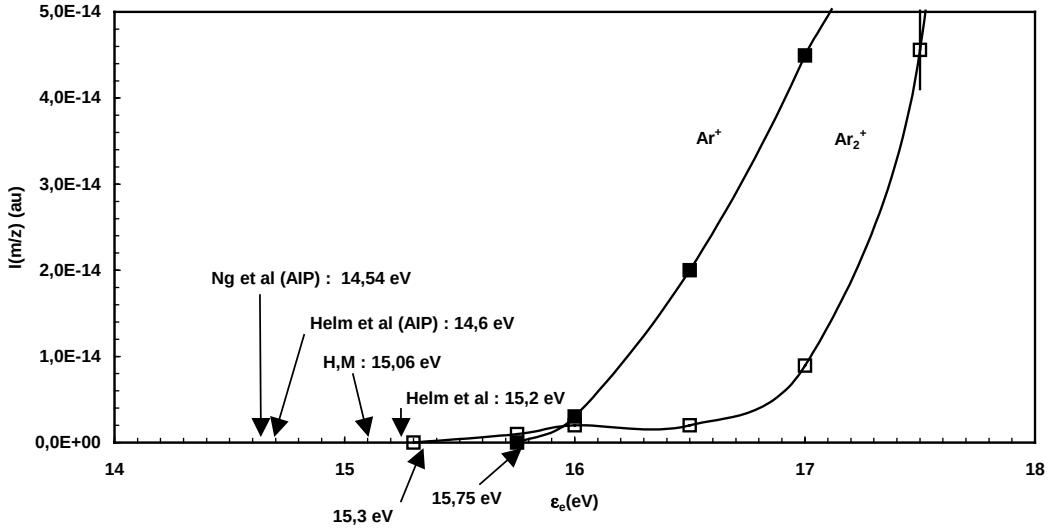

Fig. 3. Threshold ionisation: change in the signal intensity measured for $m/z = 40$ and 80 for Ar^+ and $Ar_2{}^+$, respectively, vs. the electron energy used in the ionisation chamber. Curves are polynomial interpolations with a correlation coefficient equal to 0.950.

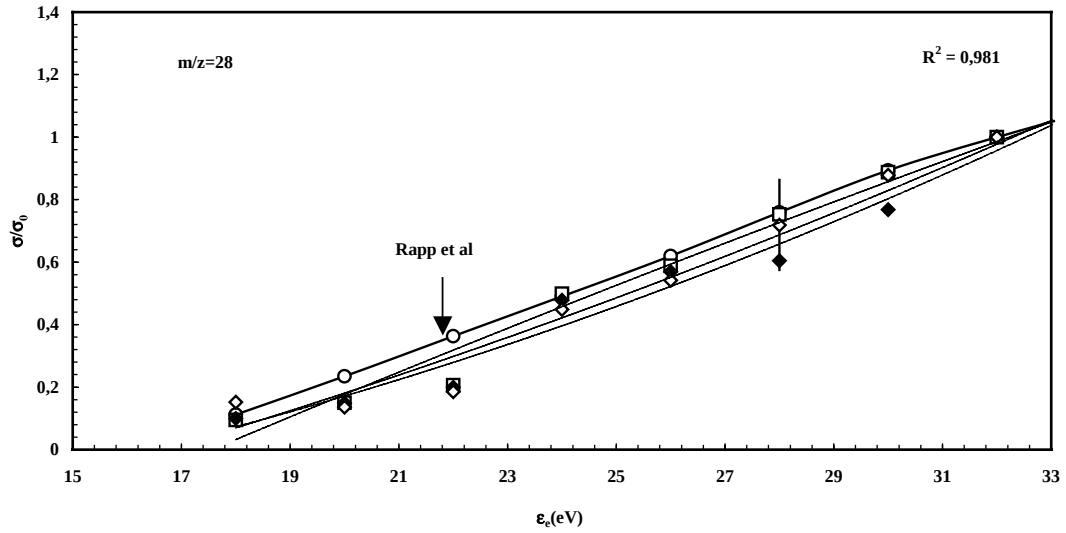

Fig. 4. The ionisation cross-section values determined for N_2 ($m/z = 28$) vs. the electron energy. Measurements are performed at different pressures range between 6×10^{-3} and 55 Pa (the full diamond is corresponding to $P = 10$ Pa, the empty diamond to 55 Pa and the empty square to 6×10^{-3} Pa). Comparison is made with the values given in the literature (Rapp and Englander-Golden [14] (empty circle)).

electron impact ionisation cross-section of N_2 producing N_2^+ at different pressures ranges between 6.10^{-3} and 55 Pa, then we compare these values to values given in the literature [14]. Results are shown on the Fig. 4, values are normalised with the reference value at 32 eV. Polynomial interpolation curves corresponding to a correlation coefficient $R^2 = 0.981$ are reported on the Fig. 4. Assuming that the error on the mass spectrometer signal intensity value is equal to 10%, the error performed on the cross-section value is equal to 20%. A good agreement is observed between our measurements and the values given in the literature. The absolute value of the cross-section can be deduced if we know the cross-section value at a given electron energy. In the case of clusters reliable values are particularly scarce for electron impact ionisation processes. The collision interaction of an electron with a comparatively weakly bounded cluster can result in the break of the cluster rather than in the ionisation. This is certainly true for van der Waals clusters at high electron energy.

Helm et al. [6] suggest that in a first approximation the ionisation cross-section for a diatomic molecule can be considered as the sum of the ionisation cross-section of the individual partners. In the case of the direct ionisation of homonuclear dimer, the potential energy diagram shows that the ionisation can proceed via six different mechanisms. Four of them are corresponding to the direct ionisation of the dimer and two are corresponding to dissociative ionisation process from intermediate repulsive states. Consequently, the ionisation cross-section must be weighted with the factor 4/6. Thus, the ionisation cross-section for the dimer Ar_2 is equal to 4/3 time the ionisation cross-section of the monomer Ar.

The Deutsch–Märk formalism (D–M formalism) determined in the case of the simple ionisation of the ground state by electron impact also has been applied to the calculation of the ionisation cross-section of small clusters [17,18].

In recents papers, authors [17,18] report an alternate approach to the microscopic D–M formalism. They use a modified additive rule including a "defect concept" to account for the fact that a cluster consisting of n atoms is not a simple collection of n atoms. This "defect concept" is explained and developed in the reference [17] and in references therein. The ionisation cross-section $\sigma(X_n)$ of a clusters X_n is expressed in terms of the ionisation cross-section $\sigma(X)$ of the constituent atom X using the relation:

$$\sigma(X_n) = n^{(1-\Delta)}\sigma(X) \tag{8}$$

The quantity Δ is called the "defect" and is nuclear charge (Z) depending. In the case of Ar, the "defect" $\Delta = 0.1$. Consequently, the ionisation cross-section for the dimer Ar_2 can be deduced from the ionisation cross-section of the monomer Ar using the relation:

$$\sigma\left(\frac{Ar_2^+}{Ar_2}\right) = 1.866\sigma\left(\frac{Ar^+}{Ar}\right) \tag{9}$$

Good correlations have been obtained by Deutsch et al. [17,18] between experimental results and theoretical calculations using this new formalism ("defect concept") in the cases of the ionisation cross-section of Br_2, I_2, C_2, C_3 and Ag_n ($n = 2$–7).

The electron impact ionisation values of Ar_2 determined using the method proposed by Helm et al. [6] are 40% lower than the values calculated using the "defect concept" of Deutsch et al. [17,18]. At 32 eV the direct ionisation cross-section given for Ar is 1.967×10^{-20} m^2 [14] and using (9) it can be estimated equal to 3.67×10^{-20} m^2 for Ar_2.

The Fig. 5 shows the ionisation cross-section of Ar_2 producing Ar_2^+ and of Ar producing Ar^+ versus the electron

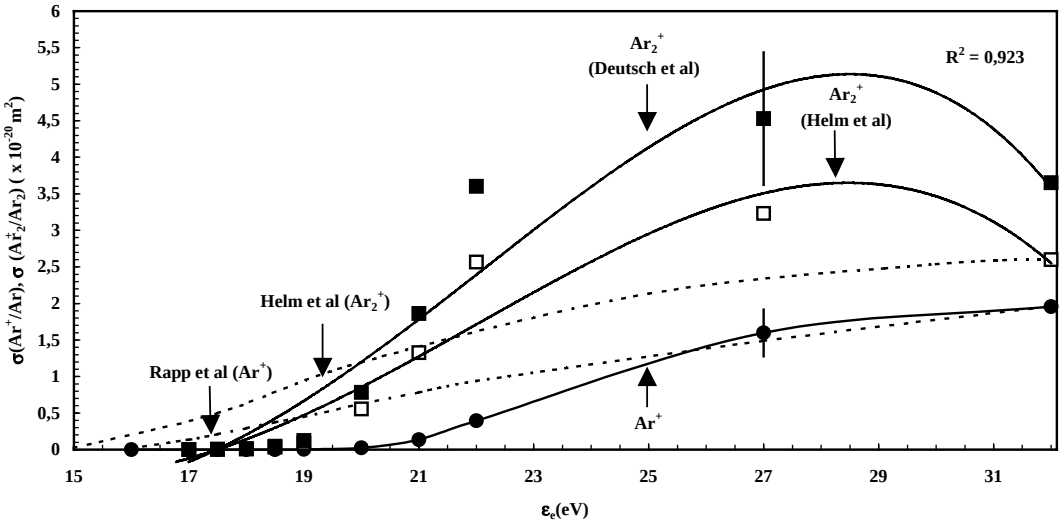

Fig. 5. Electron impact ionisation cross-section of Ar_2 producing Ar_2^+ and of Ar producing Ar^+ vs. the electron energy. The values are compared with values given in the literature. Rapp et al. [14] for Ar and Helm et al. [6] for Ar_2 (dashed curves). In this figure, the empty squares correspond to results obtained using the method proposed by Helm et al. [6] and the full squares correspond to results obtained using the method proposed by Deutsch et al. [17].

energy value. In the case of Ar_2, results obtained using the two methods (Helm et al. [6] (empty square) and Deutsch et al. [17] (full square)) are compared. The figure shows also the cross-section values given in the literature Rapp and Englander-Golden [14] for Ar and, Märk [8] and Helm et al. [6] for Ar_2 (dashed curves). The cross-section values determined using (7) for Ar_2 or Ar are given with an estimated error equal to 20%.

A polynomial interpolation corresponding to a correlation coefficient equal to 0.923 is reported both in the case of Ar and Ar_2. Our results are close to the values given in the literature. For the ionisation of Ar_2 the curve shows a maximum at about 28 eV. This maximum is also observed by Märk [8] and Helm et al. [6]. It can be ascribed to the effect of the dissociation of Ar_2 when it is ionised producing Ar^+. This dissociative ionisation process is very efficient at large electron energy values (>28 eV). In his reviews article Märk [8] gives the ionisation fragmentation ratio of small van der Waals clusters at 100 eV. In the case of Ar_2 experimental results shows that the fragmentation ratio gives 40% of Ar^+ and 60% of Ar_2^+ and theoretical calculations based on the potential energy curves predict 33% of Ar^+ and 67% of Ar_2^+. We have limited our measurement to low electron energy values (until 32 eV) in order to measure only the direct ionisation cross-section of the dimer and to prevent from the dissociative ionisation of Ar_2.

As it was previously discussed the Ar^+ ion can be produced by the direct ionisation process of argon atoms or by the dissociative ionisation process of Ar_2 dimer. Also the metastable decay processes of Ar_n^+ ion clusters can produce Ar^+. Scheier et al. [19] have studied the metastable decay of Ar_3^+ ion into Ar^+ ion they have shown that this phenomena proceed predominantly via a sequential decay series involving a multiple monomer fragmentation patterns.

$$Ar_3^+ \xrightarrow{k_{3,2}} Ar_2^+ + Ar$$

$$Ar_2^+ \xrightarrow{k_{2,1}} Ar^+ + Ar$$

They show that the Ar_3^+ decay in Ar_2^+ ion is less efficient than the Ar_2^+ decay in Ar^+ ion: $k_{3,2} = 45\,s^{-1}$ and $k_{2,1} = 680\,s^{-1}$ that corresponds to the following time constant $\tau_{3,2} = 0.02$ s and $\tau_{2,1} = 0.0015$ s.

In a first approximation, the metastable decay from the ionisation chamber to the detector can be described using an exponential law [19]:

$$Ar_n^+ = Ar_{n0}^+ \exp\left(\frac{-t}{\tau_i}\right) \quad (10)$$

where Ar_{n0}^+ is the density of Ar_n^+ ion at the ionisation chamber and Ar_n^+ is the density after a transit time t across the quadrupole.

Assuming that the velocity of the species into the quadrupole is at least equal to the velocity before the expansion, i.e. $v = 398$ m/s at 300 K, the time corresponding to the travel of the species from the ionisation chamber to the detector (0.4 m) is lower than 10^{-3} s. Because of the expansion effect, this velocity after the nozzle (B) is expected to be larger and, consequently, the transit of the species trough the quadrupole is probably lower than 10^{-3} s.

So the density of Ar_2^+ at the detector is at least equal to 51% of the density in the ionisation chamber and the density of Ar_3^+ at the detector is at least 95% the density in the ionisation chamber. Consequently, the contribution of Ar_2^+ decay to the formation of Ar^+ is expected to be efficient but that of Ar_3^+ is too low and not efficient to produce Ar_2^+ ion. The metastable decay is probably less efficient in the case of larger ion clusters Ar_n^+ because each successive fragmentation is produced simultaneously to the additional

cooling of the remaining complexes that leads to a lowering of the rate for further evaporations.

In our case, the mass spectrometer measurements shows none peak corresponding to Ar_3^+ ion at $m/z = 120$. According to the literature [18], the fact that the trimer ions peak is extremely low does not means that no neutral trimer species are within the expanding beam because the neutral trimer can be largely dissociated in the ionisation chamber producing Ar_2^+. According to Märk [8], the electron ionisation fragmentation ratios of Ar_3 according to the reaction:

$$X_n + e \rightarrow X_m^+ + 2e + (n-m)X$$

And given by the relation $f(n/m) = (X_m^+)/\Sigma_{(l=1,n)}(X_l^+)$, (where (X_m^+) is the density of the X_m^+ ions and $\Sigma_{(l=1,n)}(X_l^+)$ is the sum of the density of all the different cluster ions) are at an electron energy equal to 100 eV, $f_{3,1} = 0,3$, $f_{3,2} = 0,7$, $f_{3,3} < 10^{-4}$. These values are expected to be lower at a lower electron energy.

Moreover, according to Golomb and Good [21] the contribution of large neutral clusters is relatively small compared to the contribution of monomer and dimer to produce Ar^+ or Ar_2^+. These authors found that at a pressure equal to 10^5 Pa and a temperature equal to 300 K, the signal intensity values measured for $m/z = 400$, 120, 80 and 40 are ranges between 0.5 and 1 au, 1 and 10 au, 10 and 100 au, 10 and 100 au, respectively, when the nozzle diameter is equal to 0.117 cm and between 0.1 and 1 au, 1 and 10 au, 100 and 1000 au for $m/z = 120$, 80 and 40, respectively, when the nozzle diameter is equal to 0.034 cm. In our case, the nozzle diameter is smaller ($d = 0.01$ cm) as well as the pressure in the first cell is lower, $P = 100$ Pa. The conditions of constant cluster size for supersonic nozzles show that the cluster size is depending on the scaling law $Pd^{0.55} =$ constant [8]. So, to obtain the same cluster size distribution, the pressure should increase with decreasing nozzle diameter. Consequently, in our case the cluster size distribution is expected to be smaller than the distribution obtained by Golomb and Good [21] and the contribution of large neutral clusters to the formation of Ar^+ or Ar_2^+ can be neglected in comparison to the contribution of Ar and Ar_2. The fragmentation of large neutral cluster and specifically of Ar_3 in Ar_2^+ are probably not efficient and thus does not affect the value measured for the ionisation of Ar_2 in Ar_2^+. These conclusions are confirmed by the results given by Dehmer and Pratt [22]. With a free supersonic molecular beam in pure argon at room temperature expanded through a 10–12 μm diameter orifice, they have shown that the dimer can be prepared in the beam over a wide range of pressure (lower than 4 atm) where the presence of larger clusters is not detectable. The beam is only composed with Ar and Ar_2 species.

To conclude, these different remarks show that the contribution of Ar_3 and of larger clusters to produce Ar_2^+ can be neglected and the most important contribution to produce Ar^+ after the direct ionisation of Ar is probably the dissociative ionisation process of Ar_2. The contribution of metastable decay processes are probably lower than the contribution of the former processes. Thus, the consideration on the various reactive processes shows that most of Ar_2^+ ions result probably of the direct ionisation of Ar_2 neutral dimer clusters.

4. Conclusion

This work is devoted to the study of the Ar_2 dimer clusters produced in a pure argon after an adiabatic expansion through a 100 μm diameter hole. Study is performed using a mass spectrometer. We have measured the threshold ionisation of Ar_2 and show that Ar_2^+ formation proceed mainly via the direct ionisation of the neutral dimer. The contribution of other processes to the ionisation like the dissociative ionisation process of larger clusters or the Hornbeck–Molnar process are low in comparison to the contribution of the direct ionisation of Ar_2 and can be neglected. We have measured the absolute total ionisation cross-section value of Ar_2 and Ar at low electron energy (lower than 32 eV) in order to limit the effect of the dissociation ionisation of the dimer. The absolute value of the electron impact ionisation cross-section of Ar_2 has been determined using an alternate approach of the D–M formalism including the "defect concept". Results are compared to the values given in the literature.

The curve of the ionisation cross-section of Ar_2 producing Ar_2^+ shows a maximum at about 28 eV. For larger electron energy values, the decrease of the ionisation cross-section can be ascribed to the fragmentation of Ar_2 cluster when they are ionised.

We have characterized the dimer source (see Appendix B) and shown that the dimer concentration in the expansion strongly increases at a total pressure in the first cell larger than 700 Pa. At a lower pressure, the dimer concentration is vanishing and remains nearly unchanged. The percentage of Ar_2 produced is equal to 0.5% at a stagnation pressure equal to 1100 Pa.

Such a source can be used in order to study the reactivity of the dimer neutral argon with other atoms, molecules or radicals.

Appendix A. Characterization of the expansion jet after the nozzle

Molecular beam sources are characterized by the Knudsen number, defined as the ratio of the mean free path λ_0 in the first vacuum cell to the sample hole diameter (nozzle diameter) D [7], $K_n = \lambda_0/D$.

In our case at $P_1 = 133$ Pa, the mean free path is about 5×10^{-5} m and the Knudsen number is equal to 0.5 so the flow through the nozzle [7] is not effusive and consequently the particles undergoes many collisions passing through the sample hole. These collisions during the hydrodynamic expansion [8] give rise to a cooling of the jet producing the condensation of species via a super saturation process. This

method of adiabatic expansion is commonly employed in order to produce rare-gas clusters. It involves the expansion of the gas from a pressurized source through a narrow opening into an expansion chamber of lower pressure [1,2,3,8,10–14].

The expansion is characterized by the Mach number [8,9], defined as the ratio of the flow speed (u) to the sound speed (c) as:

$$M = \frac{u}{c} \tag{A.1}$$

where $c = (\gamma RT_2)^{1/2}$, $\gamma = C_p/C_v = 5/3$ for a perfect gas.

In an adiabatic expansion, the energy conservation is written using the balance equation:

$$C_{p1}T_1 = \frac{u^2}{2} + C_{p2}T_2 \tag{A.2}$$

T_1, T_2, C_{p1}, C_{p2} are the temperature and the heat capacity before and after the expansion, respectively. Assuming that $C_{p1} = C_{p2} = C_p$, the Mach number can also be written as:

$$M = \left(\frac{2C_p\Delta T}{\gamma RT_2}\right)^{1/2} \tag{A.3}$$

Using the relation for adiabatic systems:

$$\left(\frac{P_2}{P_1}\right)^{\gamma-1} = \left(\frac{T_2}{T_1}\right)^{\gamma} \tag{A.4}$$

the Mach number becomes:

$$M = \left[\left\{\frac{2}{\gamma-1}\left(\left(\frac{P_1}{P_2}\right)^{(\gamma-1/\gamma)} - 1\right)\right\}\right]^{1/2} \tag{A.5}$$

After the nozzle B the pressure in the second vacuum cell ranges from 1 to 0.1 Pa. If the pressure in the first cell is 100 Pa, the Mach number ranges between 4 and 7. Consequently this is a supersonic adiabatic expansion. Theoretically the adiabatic expansions are efficient cooling processes. Using the relation (A.4) for adiabatic systems and assuming the temperature in the first cell equal to 300 K and that $P_1 = 100$ Pa and $P_2 = 0.1$ Pa, the temperature after the expansion in the second cell is theoretically equal to 19 K. In reality this temperature is larger because the pressure in the expanding jet is probably larger than it is theoretically predicted.

Because of the sudden cooling an atomic or molecular beam containing clusters is produced when the gas expands after the nozzle. The gas through the nozzle converts the thermal energy in the high pressure source into a directed beam velocity u, producing a cooling which promotes condensation.

Appendix B. Characterization of the dimer source

It is now possible to determine the efficiency of this "mass spectrometer" dimer source, using the former results concerning the ionisation cross-section values of Ar_2.

At a pressure ranges from 1 to 2 Pa in the first cell, the Knudsen number ranges from 20 to 50. It is larger than 10 and must be considered as an effusive flow [7,8]. The argon flux through the orifice can be written as:

$$\Phi = \tfrac{1}{4}n\upsilon S_\Phi \tag{A.11}$$

where υ is the thermal velocity, n the argon density and S_Φ the orifice area.

In a first approximation neglecting, the effect of the adiabatic expansion by considering $T_1 = T_2$, so that the gas velocity in the second cell is equal to the gas velocity in the first cell. Assuming that after the nozzle the gas expands quickly in the total volume of the second vacuum cell with an internal diameter $D = 50$ mm and a surface area S. The total pressure back to the expansion is given by the relation:

$$P_T = \frac{1}{4P_{To}}\frac{S_\Phi}{S} \tag{A.13}$$

P_{To} is the total pressure in the first cell.

Under these conditions the total pressure after the expansion can be roughly estimated using the relation $P_T = 10^{-6} \times P_{To}$.

Assuming in a first approximation that at a low pressure $P_T = P_{Ar}$, it is possible to deduce P_{Ar} from the mass spectrometer measurements using:

$$P_{Ar} = \alpha I(Ar^+) \tag{A.14}$$

where $\alpha = 1/(3 \times 10^{-7})$ Pa/A, determined from the experimental results obtained at low pressure (at a Knudsen number larger than 10).

The Ar_2 partial pressure in the expansion can be deduced from mass spectrometer measurements assuming that the Ar^+ and $Ar_2{}^+$ ions results mainly from direct ionisation processes. So it is necessary to work at a low electron energy (18 eV in our case).

Because of the low pressure in the ionisation chamber, we suppose that the transmission factor for both ions Ar^+ and $Ar_2{}^+$ remains unchanged all over the pressure range under investigation and that they are equal. This last assumption is true only for large m/z ratio ($m/z > 10$) [20]. Using Eq. (9), the partial Ar_2 pressure in the ionisation chamber is given by:

$$P(Ar_2) = 0.53\left(\frac{I(Ar_2{}^+)}{I(Ar+)}P_{Ar}\right) \tag{A.15}$$

The Fig. 6 shows the Ar and Ar_2 partial pressure in the ionisation chamber versus the total pressure in the first cell. The relative error realised on the pressure values is determined from error calculations on (A.15) and assuming a relative error on the mass spectrometer intensity values equal to 10%. It can be seen that the Ar partial pressure increases with the total pressure in the first cell increasing. However, the Ar_2 partial pressure remains constant until 700 Pa and strongly increases for larger pressure values. This behaviour can be explained by the cooling effect due to the expansion, more efficient at large pressure.

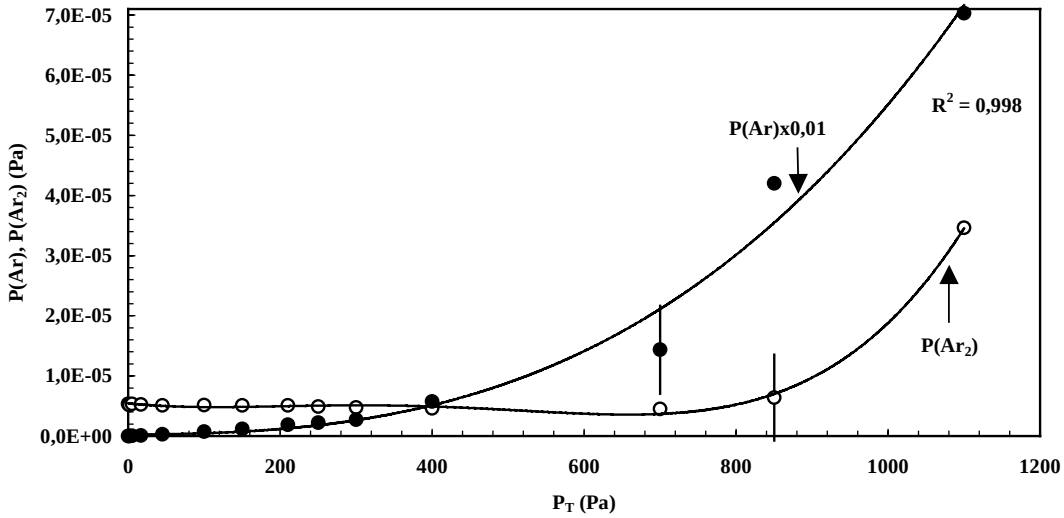

Fig. 6. The partial pressures of Ar and Ar_2 vs. the total stagnation pressure in the first cell.

The Ar_2 partial pressure is about 0.5% of the total pressure in the expansion chamber at a stagnation pressure equal to 1100 Pa.

References

[1] R.A. Zahoransky, J. Hoschele, J. Steinwandel, J. Chem. Phys. 103 (20) (1995) 9039.
[2] E. Hendell, U. Even, J. Chem. Phys. 103 (20) (1995) 9045.
[3] R.G. Keesee, A.W. Castelman Jr., in: E.R. Berstein (Ed.), Studies in Physical and Theoretical Chemistry, vol. 69, Elsevier, Amsterdam, 1990, p. 507.
[4] N.E. Levinger, D. Ray, M.L. Alexander, W.C. Lineberger, J. Chem. Phys. 89 (9) (1988) 5654.
[5] S. Neeser, T. Kunz, H. Langhoff, J. Phys. D: Appl. Phys. 30 (1997) 1489.
[6] H. Helm, K. Stephan, T.D. Märk, Phys. Rev. 19 (6) (1979) 2154.
[7] W.L. Hsu, D.M. Tung, Rev. Sci. Instrum. 63 (9) (1992) 4138.
[8] T.D. Märk, Int. J. Mass Spectrom. Ion Process. 79 (1987) 1.
[9] C. Nordling, J. Osterman, Physics Handbook, Studenlitteratur und Sweden, 1988.
[10] N.E. Levinger, D. Ray, M.L. Alexander, W.C. Lineberger, J. Chem. Phys. 89 (9) (1988) 5654.
[11] P. Scheier, A. Stamatovic, T.D. Märk, J. Chem. Phys. 89 (1) (1988) 295.
[12] Z.Y. Chen, C.D. cogley, J.H. Hendricks, B.D. May, J. Chem. Phys. 93 (5) (1990) 3215.
[13] O.F. Hagena, W. Obert, J. Chem. Phys. 56 (5) (1972) 1793.
[14] D. Rapp, P. Englander-Golden, J. Chem. Phys. 43 (5) (1965) 1464.
[15] H. Toyoda, H. Kujima, H. Sugai, App. Phys. Lett. 54 (1989) 1507.
[16] J. Roboz, Introduction to Mass Spectrometry, Interscience, NY, 1984.
[17] H. Deutsch, K. Becker, T.D. Märk, Eur. Phys. J. D 12 (2000) 283.
[18] H. Deutsch, J. Pittner, V. Bonacic-Koutecky, K. Becker, S. Matt, T.D. Märk, J. Chem. Phys. 111 (5) (1999) 1964.
[19] P. Scheier, A. Stamatovic, T.D. Märk, J. Chem. Phys. 89 (1) (1988) 295.
[20] J.L. Jauberteau, L. Thomas, J. Aubreton, I. Jauberteau, Plasma Chem. Plasma Process. 18 (1) (1998) 137.
[21] D. Golomb, R.E. Good, J. Chem. Phys. 52 (3) (1970) 1545.
[22] P.M. Dehmer, S.T. Pratt, J. Chem. Phys. 76 (2) (1982) 843.